

## Synthesis And Characterisation Of Psidium Guajava - Iron Nano Particles (PG-Fenps)

Thanusha Punugoti<sup>1\*</sup>, Meena Vangalapati<sup>2</sup>

### Abstract.

In recent years, green process techniques have reached modest impact ailments and are nontoxic precursors, and they are emphasised in the advancement of nanotechnology. Psidium guajava leaf extract was employed to make ecologically friendly iron nanoparticles in this study. The function of iron nanoparticles is studied using FTIR, SEM, and XRD methods. This study used the adsorption approach to remove a textile dye (Crystal violet) from an aqueous solution under various contact duration, pH, beginning dye concentration, adsorbent dose, and temperature parameters. The adsorption tests were carried out in batches.

**Keywords:** Nano technology, textile dye, SEM, XRD, FTIR.

### 1.Introduction

Nanotechnology is a very young and rapidly evolving technology with several practical applications. Nanotechnology may be created using both bottom-up and top-down approaches [1]. Using deposition or reduction settings, atoms and molecules combine in a bottom-up process to form nanoparticles of the desired size and shape. Top-down, on the other hand, removes atoms and molecules from bulk materials using the reverse process [2,3,4]. Nanotechnology has the capacity to measure, modify, and manufacture objects at the atomic level between 1 and 100 nanometers. This has a very high surface area to volume ratio. Bottom-up nanoparticle biosynthesis is a kind of nanoparticle biosynthesis in which the reaction occurs in reduction or oxidation [5].

Physical and chemical procedures are commonly used to make nanoparticles, which are toxic and can cause death as well as harm to the environment and living things [6,7]. Metal nanoparticles are produced in a number of techniques, including anodization, wet oxidation, heating, hydrothermal, and sonication [8,9], all of which are costly and potentially detrimental to the environment. Green synthesis is a method of substituting a natural extract, such as tree leaves, for the reducing agent. Green synthesis is less costly, more ecologically friendly, and does not require high temperatures or pressure as compared to chemical and physical procedures. This procedure does not utilise any dangerous chemicals. Green synthesis nanoparticles are inexpensive and dependable. Phenolics, polysaccharides, and flavonoids with redox characteristics are examples of secondary metabolites found in plants. Psidium guajava leaves, for example, create Fe nanoparticles, which function as a reducing and capping agent [10,11]. Coffee and tea polyphenols are among the substances used to manufacture nZVI. These chemicals are created in a unique method. They're non-toxic and biodegradable, and they're made from natural materials.

Iron metal particles that are smaller than a micrometre in size are known as nanoscale iron particles. They are very reactive due to their large surface area[12]. In the presence of oxygen and water, as well as nanoparticles, it is even quicker than in bulk material. They oxidise fast and release free iron ions[13,14]. They're commonly employed in medical and laboratory settings, and they've also been researched for the cleanup of chlorinated organic compound-contaminated industrial sites. This

---

<sup>1\*</sup>B.Tech Student, Department of Mechanical Engineering, AUCE(A), Visakhapatnam, 530003, AP, India. thanushachowdary123@gmail.com,

<sup>2</sup>Professor, Department of Chemical Engineering, AUCE(A), Visakhapatnam, 530003, AP, India. meenasekhar2002@yahoo.com

property restricts its application in inert conditions [15, 16]. Nanoparticles of iron are non-toxic. They are naturally superparamagnetic [17]. Magnetite and its oxidised counterpart, maghemite, are the two most common types. They have a wide range of uses in biological imaging, heavy electrical, catalysis, and critical chemical processes because to their superparamagnetic nature..

## 2. Materials and Methods

### 2.1 Preparation of *Psidium guajava* leaves extract:

The leaves of *Psidium guajava* were harvested. By adding the appropriate leaves extract to FeCl<sub>3</sub> solutions, iron nanoparticles were created. Individual extracts of the leaves were made using 10 grams of leaves. The conical flask is filled with 100ml of Deionized water and 10 grams of leaf extract is added to the flask. The mixture should be cooked for 10 minutes at 80°C. When the mixture has reached room temperature, filter it through what's man filter paper. This filtrate can be stored at 4°C for up to a week and then utilised.



Fig-1. *Psidium guajava* Leaves

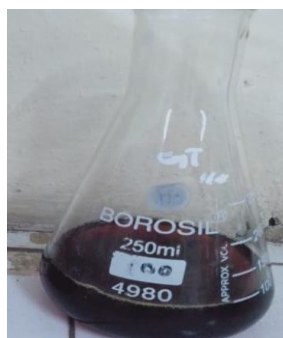


Fig-2. *Psidium guajava* extract

### 2.2 Synthesis of iron nanoparticles:

Iron nanoparticles were created by adding FeCl<sub>3</sub> to *Psidium guajava* leaves extract. In 500mL of water, dissolve 8.11 grams of FeCl<sub>3</sub> granulate. This should be in a 1:1 ratio to the amount of *Psidium guajava* leaves extract produced after filtering. At room temperature, the mixture should be stirred using a mechanical stirrer. The reduction of Fe<sup>+2</sup> ions is predicted by the rapid appearance of a black precipitate. As a result, the precipitates were centrifuged at 5000 rpm for 20 minutes. The iron nanoparticles were finally dried for 3 hours at 65 degrees Celsius in a vacuum oven.



Fig-3. Synthesized PG-Fe



Fig-4 Centrifuged PG-FeNP



Fig-5. Dried FeNP

## 2.3 PG-FeNP Characterization

### A) Scanning Electron Microscope (SEM):

scanning electron microscope (SEM) is an electron microscope that uses a focussed stream of electrons to scan the surface of a sample to obtain pictures. When electrons contact with atoms in a sample, they produce a variety of signals that carry information about the sample's surface topography and composition. A raster scan pattern is used to scan the electron beam, and the position of the beam is coupled with the intensity of the received signal to create a picture. Secondary electrons generated by atoms stimulated by the electron beam are detected using a secondary electron detector in the most common SEM mode (Everhart-Thornley detector). The quantity of secondary electrons that may be detected, and hence the signal strength, is influenced by specimen topography, among other factors. The resolution of a scanning electron microscope (SEM) is better than 1 nm.

### b) X-Ray Diffraction (XRD):

X-ray diffraction (XRD) uses the dual wave-particle duality of X-rays to gain information on crystalline materials' structure. The approach is primarily used to identify and characterise chemicals based on their diffraction patterns.

### (c) Fourier Transform Infrared Spectroscopy (FTIR):

Fourier transform infrared spectroscopy (FTIR) is a technique for obtaining an infrared spectrum of a solid, liquid, or gas's absorption or emission. An FTIR spectrometer captures high-spectral-resolution data over a large spectral range at the same time. This gives it a big advantage over a dispersive spectrometer, which only measures intensity across a small range of wavelengths at a time.

## 3. Discussion and Conclusions

### 3.1 Scanning Electron Microscope (SEM) Images:

The SEM (Scanning Electron Microscope) images in Figures 6 and 7 clearly reveal the tiny structures and varying sizes of PG-FeNP. For optimal imaging, it delivers high resolution and steady probe currents. The nanoparticles generated ranged in size from 159.3 to 205.6 nanometers.

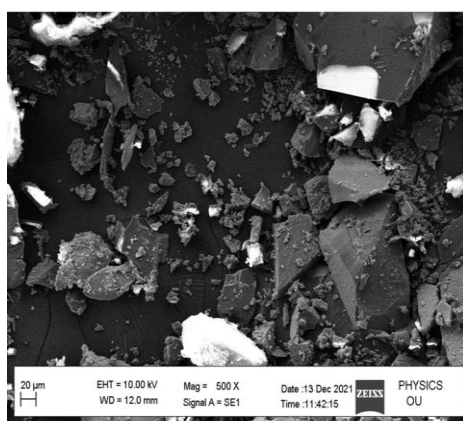


Fig -6 PG- FeNP before synthesis

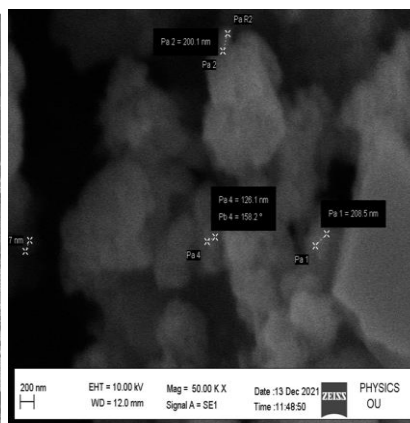
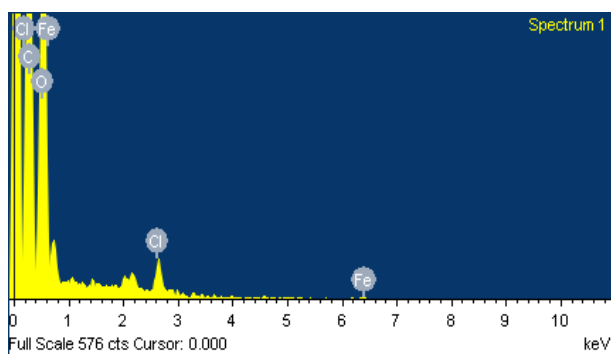


Fig-7 PG- FeNP after synthesis



**Fig-8** Graphical representation of SEM( PG- FeNP)

**3.2 X-Ray Diffraction (XRD):**

Peak positions in the Fig suggest hexagonal wurtzite crystal structure development. The maxima of PG-FeNps at 2 values are 5.740, 10.920, 17.940, 22.310, 28.520, and 30.520. Figure 9 shows the XRD for PG-FeNps

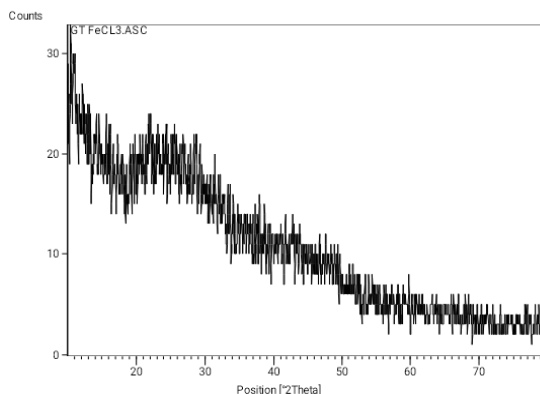


**Fig-9** XRD pattern of PG-FeNps

**3.3 Fourier Transform Infrared Spectroscopy (FTIR):**

Figure 10 shows the FTIR spectrum of Pure PG-FeNps. Various functional categories are represented by peaks at different places. Carboxylic, hydroxide, and C=C groups make up the majority of functional groups. Before and after FTIR, the peaks for PG-FeNps were 2400cm-1 and 2475cm-1

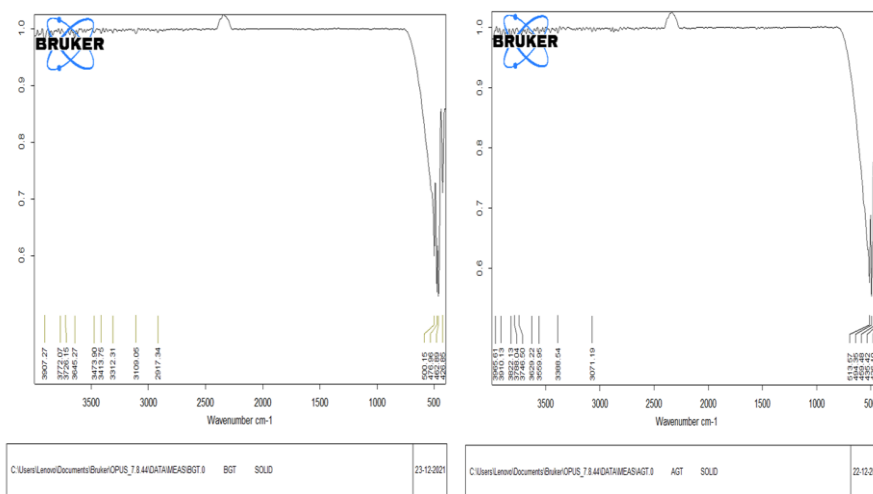


**Fig-10.** FTIR before and after analysis of PG-FeNps

To investigate the influence of various parameters on the removal of Crystal violet from an aqueous solution (made in the lab) utilising PG-FeNP as an adsorbent, experimental data is obtained in a batch mode of operation. Experiments are used to investigate the influence of various factors on the adsorption of Crystal violet, followed by a theoretical attempt to interpret the results of the graphical analysis. The current investigation includes a number of different experimental runs. The following variables were investigated:

### 3.4 Contact Time (t) Effect:

Figure 11 shows time course profiles for the adsorption of crystal violet solutions over 1, 5, 10, 20, 30, 40, 50, 60, and 70 minutes. The data acquired from the adsorption of crystal violet PG-FeNP revealed that an equilibrium adsorption needed a contact duration of 60 minutes, and there was no significant change in dye concentration with increasing contact time. As a result, the dye uptake and residual dye concentration after 60 minutes are used to determine the equilibrium values. The equilibrium duration of 60 minutes has been chosen for further investigations of adsorption with additional parameters using PG-FeNP as an adsorbent.

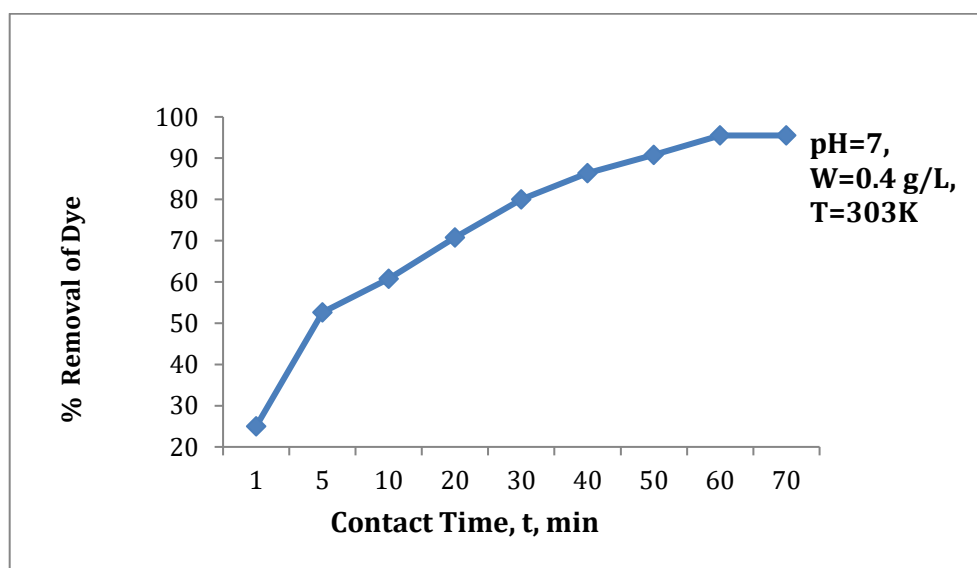


Fig-11. Effect of Dosage for adsorption of crystal violet using PG-FeNps

### 3.5 Adsorbent dose effect (W):

The adsorbent dose was changed from 0.1 to 0.5 g to evaluate the effect of adsorbent dosage on crystal violet removal while keeping the other parameters constant. The duration of interaction was 60 minutes. Figure 12 illustrates that as the adsorbent dose is increased, the % dye removal increases. For a 20 ppm dye solution, the percent dye removal rose from 86.4 percent to 96.2 percent when employing PG-FeNP. The rise in Crystal violet removal with an increase in adsorbent dose from 0.1 to 0.5 g can be ascribed to increased surface area and a high number of accessible sorption sites.

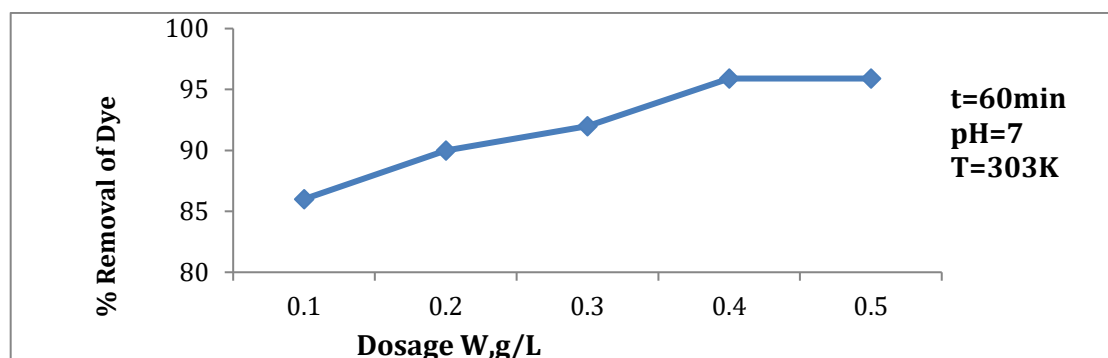
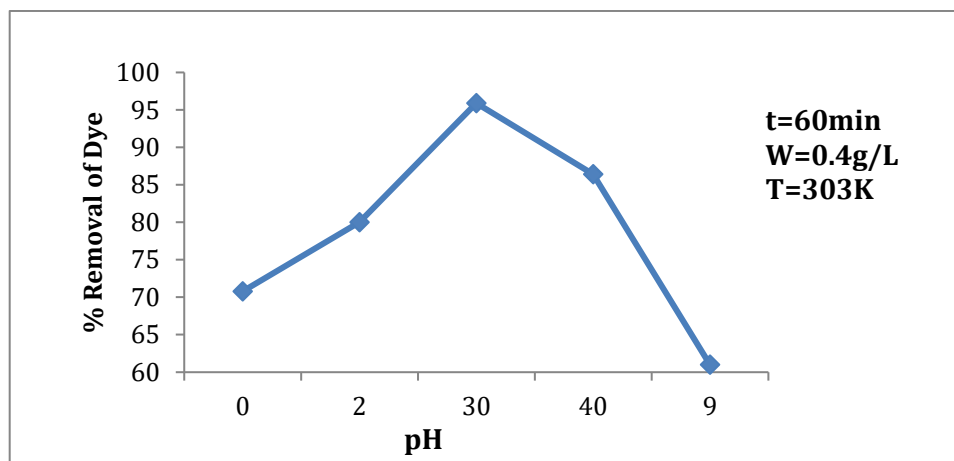


Fig-12. Effect of Dosage for adsorption of crystal violet using PG-FeNps

### 3.6 Effect of solution pH:

One of the most critical aspects determining the adsorption process is the initial pH. The effect of initial pH on crystal violet adsorption using PG-FeNP is shown in Fig 13. The proportion of dye removal increased with a rise in pH from 5 to 7, and then dropped with an increase in pH up to 9. As a result, the optimal pH was determined to be 7. At a lower pH, both hydrogen and crystal violet ions fight for adsorption, resulting in less adsorption. As the pH rises, the number of OH<sup>-</sup> ions in the solution rises, resulting in an electrical attraction between the positive crystal violet ions and the negative ions on the adsorbent, increasing the percent of adsorption.



**Fig- 13**Effect of pH for adsorption of crystal violet using PG-FeNps

### 3.7 Effect of initial concentration of aqueous dye solution (C<sub>i</sub>):

The impact of the initial dye concentration on the removal of Crystal violet dye from the solution was investigated through experiments. Figure 14 shows the percent dye removal and dye uptake as a function of initial dye concentration. The dye absorption rose as the original dye concentration grew, but the proportion of dye removed dropped as the initial dye concentration increased, as seen in the graph. With an increase in the initial dye concentration (from 10 to 100 mg/L), the driving forces, i.e. concentration gradient, rise, resulting in an increase in dye absorption. However, for PG-FeNP, the percentage of dye removed decreased from 98 to 80.8 percent. Although there was an increase in dye absorption, the decrease in percentage removal might be due to a shortage of surface area to tolerate much more dye in the solution. The proportion elimination of dye at higher concentration levels is falling, whilst the equilibrium intake of dye is increasing. Because all dye in the solution could interact with the binding sites at lower concentrations, the percentage of dye removed was greater than at higher starting dye concentrations. The saturation of adsorption sites causes reduced adsorption yield at increasing concentrations.

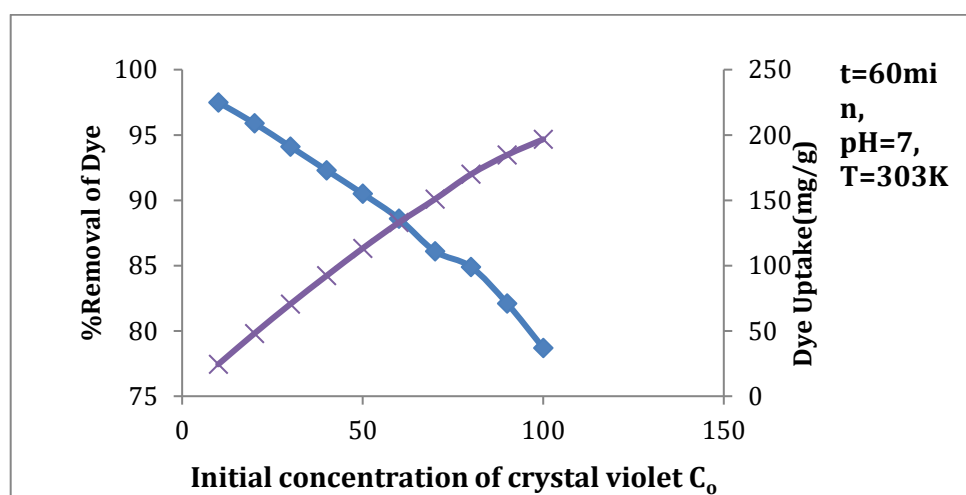


**Fig-14.**Initial concentration for adsorption of crystal violet using PG-FeNps

### 3.8 Effect of Temperature (K):

The adsorption of crystal violet by PG-FeNP at various temperatures revealed that as the temperature was raised, the adsorption capacity decreased. The adsorption process is influenced by temperature in two ways. The equilibrium capacity of the adsorbent for a given adsorbate will change as the temperature changes. Batch tests at four constant temperatures: 303, 308, 313, and 318 K were used to evaluate the influence of temperature. For the initial concentration of 20mg/L, the percent removal increased from 98.0 percent to 99.2 percent as the temperature was raised, as shown in Fig 15. This shows that the adsorption reaction is exothermic.

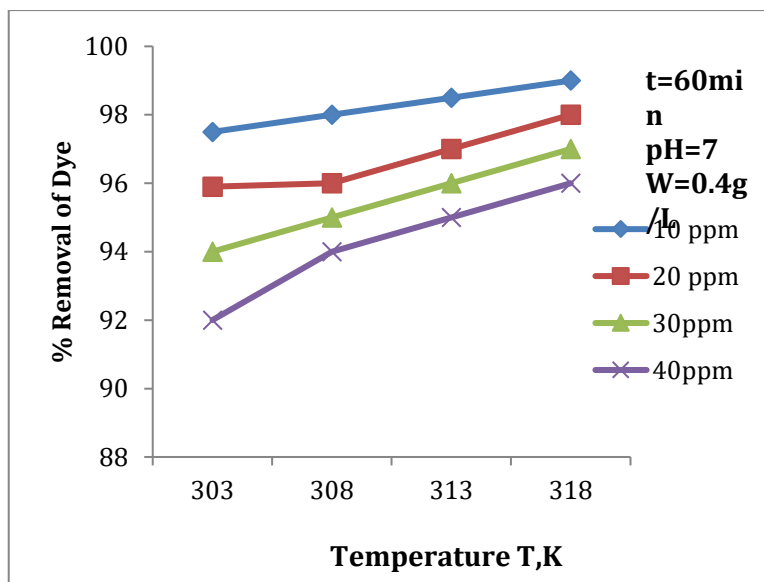


**Fig-15** Effect of Temperature for adsorption of crystal violet using PG-FeNPs

### 4. Conclusion:

For the elimination of crystal violet, which is employed as a colouring agent and disinfectant in pesticides, a simple, quick, and environmentally acceptable process is utilised to synthesis FeNPs using *Psidium guajava* leaf extracts. The removal of Crystal violet dye using PG-FeNP as an adsorbent yielded experimental results. The data were analysed for a variety of experimental runs. The following findings are drawn from the analysis. Agitation period, starting dye concentration, pH, adsorbent dose, and temperature all had a significant impact on adsorption efficacy. With increasing contact time, the % adsorption of Crystal violet increases. With an increase in adsorbent dose, equilibrium absorption dropped and percentage adsorption rose. The graph of pH vs % dye removal revealed that substantial adsorption occurred at a pH of 7. With an increase in the starting dye concentration, the percentage adsorption of Crystal violet was reduced, while dye absorption was significantly enhanced. The % adsorption of Crystal violet rose when the temperature was raised. As a result, this implies that this is a physisorption process. The current study aided in the discovery of a novel source of adsorbent for the removal of dye from effluent waste with low dye concentrations.

### 5. References:

1. Lebogang Katata-Seru, Tshepiso Moremedi, Oluwole Samuel Aremu, Indra Bahadur Green synthesis of iron nanoparticles using *Moringa oleifera* extracts and their applications: Removal of nitrate from water and antibacterial activity against *Escherichia coli*, (2018), [vol\(256\)](#), pp. 296-304.
2. Muhammad Asif Asghara, Erum Zahirb, Syed Muhammad Shahidc, Muhammad Naseem Khand, Muhammad Arif Asghare, Javed Iqbal, Gavin Walker, Iron, copper and silver

- nanoparticles: Green synthesis using green and Carica papaya leaves extracts and evaluation of antibacterial, antifungal and aflatoxin B1 adsorption activity, (2018), [Vol\(90\)](#), pp. 98-107.
3. ChandniPuriGajjalaSumana, Highly effective adsorption of crystal violet dye from contaminated water using grapheme oxide intercalated montmorillonite nanocomposite, (2018), [Vol\(166\)](#), pp. 102-112.
  4. Happy Agarwal, Venkat Kumar, Rajeshkumar, “ A review on green synthesis of zinc oxide nanoparticles –An eco-friendly approach”, Resource-Efficient Technologies, (2017), vol(3) pp.406–413.
  5. H.Jayasantha KumariP.KrishnamoorthyT.K.ArumugamS.RadhakrishnanD.Vasudevan, An efficient removal of crystal violet dye form waste water by adsorption onto TLAC/chitosan composite: A novel cost adsorbent. (2017), [Vol \(96\)](#), pp. 324-333.
  6. Bhanuprakash M. and Belagali S.L., “Study of Adsorption Phenomena by Using Almond Husk for Removal of Aqueous Dyes”, Curr. World Environ., (2017), vol.12(1), 80-88.
  7. Imtiyaz Hussain, Singh, Ajey Singh, Himani Singh, Singh, “Green synthesis of nanoparticles and its potential application” , Biotechnol Lett , (2016), vol. 38 ,pp.545–560.
  8. Sadia Saif , Arifa Tahir and Yongsheng Chen Green Synthesis of Iron Nanoparticles and Their Environmental Applications and Implications, (2016), *vol(11)*, 209.
  9. C.P. Devatha, Arun Kumar Thalla, Shweta Y. Katte, Green synthesis of iron nanoparticles using different leaf extracts for treatment of domestic waste water, (2016), [Vol\(139\)](#), pp. 1425-1435.
  10. Padmavathy, Madhu, Haseena, “A study on effects of pH, adsorbent dosage, time, initial concentration and adsorption isotherm study for the removal of hexavalent chromium (Cr (VI)) from wastewater by magnetite nanoparticles”, Procedia Technology, (2016), vol. (24), pp. 585 – 594.
  11. ChandrasekaranMuthukumaranVaiyazhipalayamMurugaiyanSivakumarMarimuthuThirumarimurugan, Adsorption isotherms and kinetic studies of crystal violet dye removal from aqueous solution using surfactant modified magnetic nanoadsorbent, (2016), [Vol\( 63\)](#), pp.354-362
  12. Shayesteh, Hadi., Rahbar-Kelishami, Ahmad., Norouzbeigi., Reza., Adsorption of malachite green and crystal violet cationic dyes from aqueous solution using pumice stone as a low-cost adsorbent: kinetic, equilibrium, and thermodynamic studies, Desalination and Water Treatment, (2016), 57 ( 27): 12822-12831.
  13. Kavitha A., Sai Pooja G. and Kaaviyavarshini M., “Colour Removal of textile dyeing effluent using Low Cost adsorbents”, International Journal of Engineering Research and General Science, (2016), vol 4(2),pp. 732-748.
  14. Jinyue Yang, Baohong Hou , Jingkang Wang, Beiqian Tian, Jingtao Bi , Na Wang, Xin Li and Xin Huang, (2019). ”Nanomaterials for the Removal of Heavy Metals from Wastewater”, nanomaterials.
  15. Kuchi Chandrika, Ashwarya Chaudhary, Tejaswi Mareedu, U. Sirisha, Meena Vangalapati, Adsorptive removal of acridine orange dye by green tea/copper-activated carbon nanoparticles (Gt/Cu-AC np), Materials Today: Proceedings, Volume 44, Part 1, (2021), Pages 2283-2289.
  16. P. VenkataRao, G. SaiTarun, Ch Govardhani, B. Manasa, P. Joel Joy, Meena Vangalapati, Biosorption of congo red dye from aqueous solutions using synthesized silver nano particles of Grevillea robusta: Kinetic studies, Materials Today: Proceedings, Volume 26, Part 2, (2020), Pages 3009-3014.
  17. P. Venkata Rao, P. Pydiraju, V. Madhuri, S. Vineeth, S. Rahimuddin, Meena Vangalapati, Removal of indigo carmine dye from aqueous solution by adsorption on biomass of Grevillea Robusta leaves, Materials Today: Proceedings, Volume 26, Part 2, (2020), Pages 3020-3023.